Stability Analysis of Hundred-Meter High Highway Embankment in Mountainous

Zhipeng Yang[1], Peng Li[2*], Guo Wang [1], Honghua Luo[1], Jie Che[1], Jiangxin Liu[2]

([1] China Overseas Construction Co., Ltd., Shenzhen 518000, China
[2]Research Institute of Highway, Ministry of Transport, Beijing 100088, China)

* Corresponding author's e-mail address: lpcumtb@163.com

Abstract. Based on a hundred-meter level high embankment in mountainous areas in China, the embankment stability is investigated by the FLAC3D finite difference numerical simulation, and the effects of fill height, slope grade, geo-fabric reinforcement, and the presence or absence of a wide platform at the base of slope on the stability are discussed. The results indicate that as the fill height increases, the safety factor of the subgrade slope stability gradually decreases. The decrease in slope grade, adding geo-fabric reinforcement and the setup of a wide platform at the base of the embankment all contribute to enhancing the stability of the embankment.

Keywords: Hundred-meter high embankment; stability; slope grade; wide platform; geo-fabric reinforcement

1 INTRODUCTION

During the construction of highways in the mountainous regions of Southwest China, it is inevitable to encounter situations that require deep cutting and high filling. High fill embankments have become one of the primary design structures for mountain highways Issues such as surface slips or overall instability of high fill embankments occur from time to time, which seriously affect the safety during construction and vehicular safety during operation, leading to significant economic losses [1-2]. Stability is one of the fundamental problems of high fill embankment projects, and numerous studies have been conducted by experts and scholars [3]. Based on the principle of limiting equilibrium and slice method, Sarma [4] developed a simple but accurate method to analyze the slope stability. Fukushima et al. [5] conducted a series of laboratory tests to investigate the stress-strain relationship of the coarse-grained fillers in a 90m high embankment and evaluated its stability with field observations of deformation and slope stability. Ning [6] investigated the variation of the subgrade stability safety factor under different material parameters, cohesion, internal friction angle, elastic modulus, Poisson's ratio, based on the limit equilibrium theory, and analyzed the sensitivity of the parameters. Chen [7] took a 72m fill height embankment as the research subject, and analyzed the effects of different factors such as water level fluctuation, ground slope gradient,

B. Yuan et al. (eds.), *Proceedings of the 2024 8th International Conference on Civil Architecture and Structural Engineering (ICCASE 2024)*, Atlantis Highlights in Engineering 33,
https://doi.org/10.2991/978-94-6463-449-5_32

and the presence or absence of geo-grids on the stability of the high embankment. Liu [8] developed a modified Duncan-Chang model through large-scale triaxial shear tests and conducted a study on the stability of high-fill embankments in complex terrain by means of three-dimensional finite element method. Guo et al. [9] conducted external appearance observation and internal quality inspections of the road embankment, and studied the stability of the high-fill embankment under different working conditions, providing a basis for the treatment of cracking diseases.

While the above-mentioned research has deepened the understanding of the stability of high embankments, there is relatively little research on the stability of ultra-high fill subgrades, especially those exceed one hundred-meter high. For this reason, this paper takes a hundred-meter level high filled embankment as the research subject and uses the FLAC3D finite difference numerical software to conduct a numerical simulation study on its stability, which can provide a reference for similar projects.

2 ENGINEERING OVERVIEW

The hundred-meter level high filled subgrade is located in a region of low to moderate mountainous relief, characterized by sloping terrain, with the natural ground cross slope ranging from approximately 1:2.6 to 1:1.3. The area is covered by a layer of gravelly silty clay, with pockets of cobble soil, which is 0 to 3.5m thick; the gravel and cobbles consist of sandstone and slate; the bedrock is strong to moderately weathered sandstone interbedded with slate, with a strongly weathered layer thickness of 9.0 to 15.0m.

This hundred-meter high subgrade is laid out along a valley. The maximum fill height at the center of the subgrade is 63.6m, with the highest side slope on the right side reaching 114.4m. A total of 13 levels of embankment are constructed from top to bottom, with each of the 1st to 12th levels having a fill height of 8m, and the 13th level with a fill height of 10m. Retaining walls are constructed at the toe of the slopes to consolidate the slope, with a height of 10m and a buried depth of 1.6m. There is soft soil distributed in parts of the base, which was replaced with rock fragments. The 1st level slope gradient is 1:1.5, the 2nd to 5th level slope gradients are 1:1.75, the 6th to 11th level slope gradients are 1:2, the 12th level slope gradient is 1:1.5, and the 13th level slope gradient is 1:1.75; platforms are set between each level, including an 8m wide platform at the base of the 7th level embankment slope, a 52.7m wide platform at the base of the 11th level embankment slope, and the platforms at the base of the remaining embankment slopes are all 2m wide. The fill material consists of tunnel muck from nearby construction, primarily composed of moderately weathered sandstone interbedded with slate. Tests show that the uniaxial saturated compressive strength ranges from 29.5 to 39.8 MPa, which corresponds to relatively soft and relatively hard rock types.

3 NUMERICAL MODEL AND FILLING SIMULATION

3.1 Model Dimensions and Material Parameters

(1) Model Dimensions.

According to the engineering overview above, a numerical model is created. The first step is using Rhinoceros software to create and optimize the mesh, followed by importing it into the FLAC3D software via the Griddle plugin to generate a three-dimensional simplified model, which is then grouped as shown in Figure 1. In the model, the base width is 640m, and the depth is 57m.

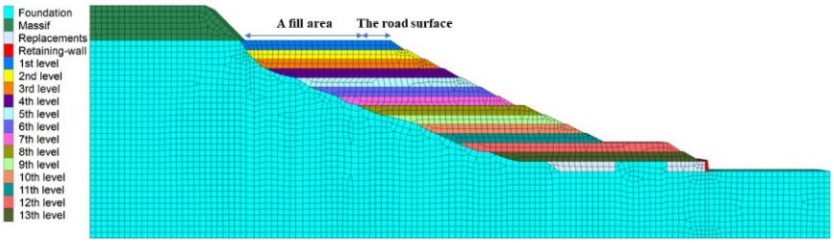

Fig. 1. Schematic of numerical model

(2) Material Parameters.

Based on geotechnical investigation data, laboratory test results and related books [10-11], the parameters for the model materials are shown in Table 1.

Table 1. Physical and mechanical parameters of materials

Category	Density (kg/m^3)	Elastic Modulus (GPa)	Poisson's Ratio	Tensile Strength (MPa)	Cohesion (MPa)	Friction Angle (°)
Massif	2200	15	0.2	2	2	40
Foundation	2200	15	0.2	2	2	40
Replace-ments	2200	15	0.2	2	2	40
Retaining-wall	2400	15	0.2	2.5	2.5	45
Embank-ment	2150	5	0.25	0.5	0.5	30

3.2 Initial Conditions

During calculation, the bottom of the model is a fixed, the four sides of the model are roller-supported, and the surface of the model is freely deformed.

Before the filling operation, the embankment grid is assigned as nulls, while the grids for the mountain, foundation, soft soil replacement at the base, and retaining walls

are assigned the corresponding materials. First, the modulus and cohesion parameters for the mountain, foundation, soft soil replacement at the base, and retaining walls are assigned infinite values for solving to ensure that the elements do not yield under the action of gravity. Then their parameters are set to the real values for calculation to further obtain the initial geostress field.

3.3 Filling Process Simulation

The filling process of the embankment for each level is simulated dynamically by gradually activating each level using the 'model null' command within the software. First, the nodal displacements and velocities generated during the initial stress calculation are zeroed out. Then, the method of graded loading is used to activate the embankment elements level by level. For each level of embankment that is filled, the mesh elements for that level are activated, and one calculation is performed, producing results for that stage of the filling. As the hundred-meter high fill subgrade has a total of 13 levels of embankment, 13 activations and calculations are required, in the sequence of the 13th level down to the 1st level of the embankment. The dynamic simulation of stage-by-stage construction allows for a better analysis of the evolution of the stability safety factor of the subgrade slope throughout the filling process.

During the stage-by-stage filling process from the 13th level to the 1st level of the embankment, the variation curve of the stability safety factor of the subgrade slope throughout the filling process is shown in Figure 2. As the filling height increases, the stability safety factor of the slope gradually decreases. After the subgrade filling is completed, the safety factor is 1.915, meeting the requirements of related specifications [12-13] for high embankment slope stability safety factor $F \geq 1.30$.

After the completion of the subgrade filling, the maximum shear strain increment cloud diagram of the subgrade is calculated using the strength reduction method, as shown in Figure 3. The maximum shear strain increment is mainly distributed from the bottom of the 1st to the 8th level of the embankment to the base, with a certain shear strain increment on the slope of the 7th level embankment, but the maximum shear strain increment does not penetrate through, indicating that the fill body is stable. Moreover, the maximum shear strain increment within the 9th to 11th level is very small, due to the fact that there is a wide platform of 52.7m at the bottom of the 11th level. The 12th and 13th levels of the embankment act as a counterweight, providing effective counter-pressure footing to the embankment above.

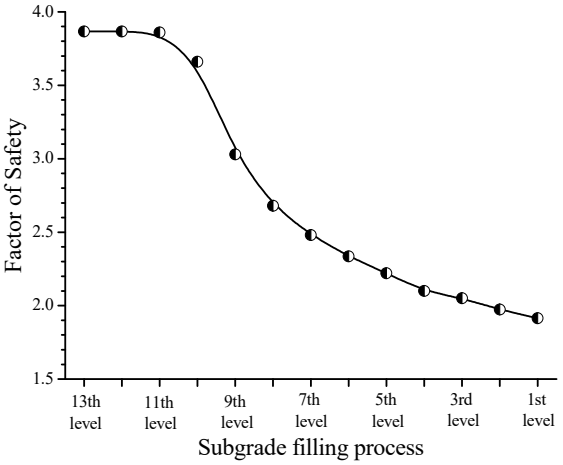

Fig. 2. Embankment slope stability during filling process

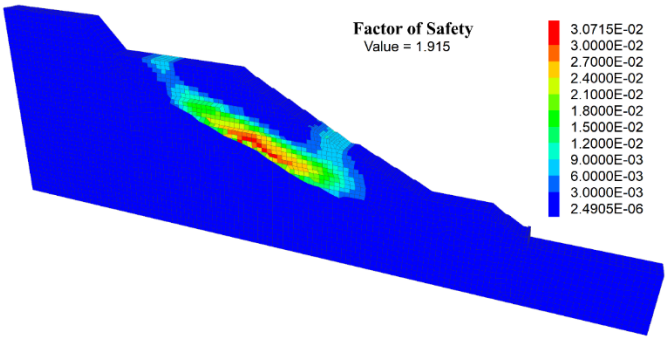

Fig. 3. Shear strain increment after the completion of filling

4 DISCUSSIONS OF INFLUENCING FACTORS

4.1 Slope Grade

The actual working conditions for the slope gradient of the subgrade are: the slope grade of the 1st level is 1:1.5, the 2nd to 5th level is 1:1.75, the 6th to 11th level is 1:2, the 12th level is 1:1.5, and the 13th level is 1:1.75. Then, all 13 levels of the embankment slope grades are set to three working conditions, respectively: 1:1.5, 1:1.75, and 1:2, and corresponding models are established. Under the premise that other conditions remain unchanged, a comparative analysis of different slope grades with the actual working conditions is conducted.

The stability safety factor for different slope grades during the filling process are shown in Figure 4. The milder the slope, the greater the safety factor. When the slope grade is 1:1.5, the stability safety factor of the embankment after filling is 1.852; when the slope grade is 1:2, the safety factor after filling is 1.961, with a difference of 0.109

between the two. While the actual working condition and when the slope grade is 1:1.75, the difference between the two is very small, with safety factors of 1.915 and 1.910, respectively. It can be seen that the change in slope grade has a certain impact on the stability safety factor of the slope, and a milder slope gradient is beneficial to improve the stability of the subgrade slope.

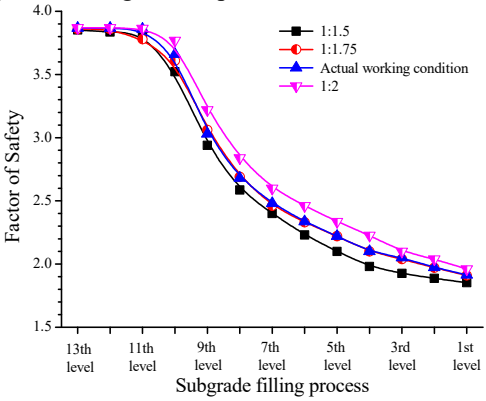

Fig. 4. Embankment slope stability indices under different slope grades

4.2 Wide Platform

In the actual working conditions, a wide platform of 52.7m is set at the bottom of the slope of the 11th level embankment. Now it has been changed to a general platform with a width of 2m with other conditions remain unchanged, a comparative analysis of having a wide platform or not is conducted.

The variation curves of the stability safety factor of the embankment with and without a wide platform during the filling process are shown in Figure 5. Without a wide platform, the stability safety factor is slightly reduced. After the filling is completed, the stability safety factor drops from the actual condition of 1.915 to 1.882 without the wide platform, a reduction of 0.033, which is a very small change.

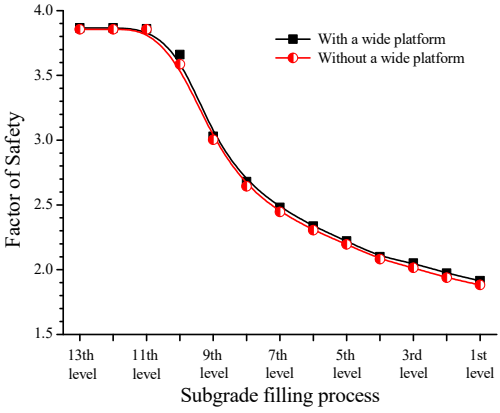

Fig. 5. Comparison of slope stability with or without wide platform

4.3 Geo-fabric Reinforcement

In the actual working conditions, there is no geo-fabric reinforcement laid in the embankment. Now it has been changed to lay a layer of geo-fabric reinforcement every 4m of embankment filling with other conditions remain unchanged, a comparative analysis of having geo-fabric reinforcement or not is conducted. And the width of the geo-fabric reinforcement is 30m, the tensile yield force per linear meter of the geo-fabric reinforcement is not less than 100kN.

The variation curves of the stability safety factor of the embankment with and without geo-fabric reinforcement during the filling process are shown in Figure 6. With geo-fabric reinforcement, the stability safety factor has been improved. After the filling is completed, the stability safety factor raises from the actual condition of 1.915 to 1.966 with the geo-fabric reinforcement, an increase of 0.051, which is also small.

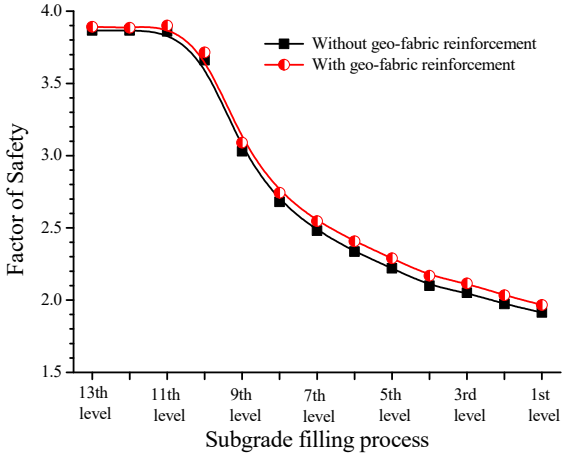

Fig. 6. Comparison of slope stability with or without geo-fabric reinforcement

5 CONCLUSIONS

In the research of the stability of super-high filled embankment on the level of one hundred meters and its influencing factors, based on the FLAC3D numerical simulation analysis, the following conclusions are drawn:

(1) As the height of the filled embankment increases, the stability safety factor decreases, signifying a negative correlation.

(2) Reducing the embankment slope grade enhances stability, suggesting design precautions should prioritize less steep slopes for higher embankments.

(3) Introducing a wide platform at the base of the embankment improves the stability of the slope above, acting as an anchorage system.

(4) Despite the observed improvement in stability from the wide platform or geo-fabric reinforcement, the change in safety factor is notably small, hinting at potential diminishing returns for either of the two measures when used solo.

The influence of actual terrain and dynamic compaction on the stability is not considered in this paper, which is somewhat different from the actual project. Therefore, the stability research on the hundred-meter high highway embankment under the actual three-dimensional terrain could be carried out in the later stage, and the beneficial effect of dynamic compaction should be also analyzed.

REFERENCES

1. Wu, L., Bian, X., Ma, X. (2015) Design and Construction of Special Soil Subgrade in Guizhou. China Communication Press Co., Ltd., Beijing.
2. Zeng, A. (2020) Discussion on Construction Technology and Disease Prevention Measures of Highway High Fill Subgrade of Expressway. Chinese & Overseas Architecture, (4): 194-196. DOI:10.19940/j.cnki.1008-0422.2020.04.062.
3. Zhu, Y., Yang, X. (2020) Analysis of Foundation Deformation and Slope Stability of High Fill Engineering. China Architecture Publishing & Media Co., Ltd., Beijing.
4. Sarma, S.K. (1973) Stability Analysis of Embankments and Slopes. Gotechnique, 23(3), 423-433. DOI:10.1680/geot.1973.23.3.423.
5. Fukushima, S., Kitajima, A., Kizawa, C., Sobue, S., Sugawara, N., Nakamura, H. (2010) Deformation Behavior and Stability of High Embankment Slope Constructed at Steep-valley (River Terrace District). Doboku Gakkai Ronbunshu, 2001, 181-200.
6. Ning, L. (2008) Study on Stability of High Rockfill Embankment. East China Jiaotong University, Nanchang.
7. Chen, P. (2011) Study on Stability of High Rockfill Embankment in Mountainous Area Highways. Railway Construction Technology, (3): 53-56, 64.
8. Liu, S. (2011) Study on Stability of High Embankment with Strong Weathering Filling under Complicated Stress Conditions. Applied Mechanics and Materials. 1448:78-84. DOI:10.4028/www.scientific.net/AMM.97-98.78.
9. Guo, Z., Yang, W., Cheng, Q. (2022) Study on Crack Disease and Stability of Slope High-fill Embankment. Subgrade Engineering, (4): 223-228. DOI: 10.13379/j.issn.1003-8825.202205016.
10. Christine, D., Roger, H. (2020) FLAC and Numerical Modeling in Geomechanics. CRC Press LLC, Florida.
11. Sun, S., Lin, H., Ren, L. (2011) Application of FLAC3D in Geotechnical Engineering. China Water & Power Press, Beijing.
12. JTG D30-2015. (2015) Specifications for Design of Highway Subgrades. China Communications Publishing & Media Management Co., Ltd., Beijing.
13. JTG/T 3610-2019. (2019) Technical Specifications for Construction of Highway Subgrades. China Communications Publishing & Media Management Co., Ltd., Beijing.